Vacuum-polarization corrections to the hyperfine-structure splitting of highly charged $^{209}_{83}$Bi ions

Leonti Labzowsky
Institute of Physics, St. Petersburg State University, Uljanovskaya 1, Petrodvorets, 198904 St. Petersburg, Russia

Andrei Nefiodov*
Theory Department, Petersburg Nuclear Physics Institute, Gatchina, 188350 St. Petersburg, Russia

Günter Plunien and Gerhard Soff
Institut für Theoretische Physik, Technische Universität Dresden, Mommsenstrasse 13, D-01062 Dresden, Germany

Pekka Pyykkö
Department of Chemistry, University of Helsinki, P.O. Box 55 (A.I. Virtasen aukio 1), FIN-00014 Helsinki, Finland
(Received 15 May 1997)

The vacuum-polarization corrections to the hyperfine structure intervals for the $2s_{1/2}$ state of $^{209}_{83}Bi^{80+}$ ion and the $2p_{3/2}$ state of Li-like, B-like, and N-like $^{209}_{83}$Bi ions are calculated. The ''dynamical'' model of the hyperfine interaction is used, in which the electron is assumed to interact with the valence proton in $^{209}_{83}$Bi nucleus via exchange of a photon. In this model, the magnetic dipole moment and the electric quadrupole moment distributions inside the nucleus are automatically taken into account. The contributions of the vacuum polarization to the hyperfine structure intervals are evaluated in the Uehling approximation. To calculate the hyperfine splittings, the Dirac-Hartree-Fock wave functions for an extended nucleus are used.
[S1050-2947(97)01312-7]

PACS number(s): 31.30.Gs, 31.30.Jv, 31.15.Ar

I. INTRODUCTION

Recently the hyperfine structure (hfs) for the ground state $1s_{1/2}$ of H-like $^{209}_{83}Bi^{82+}$ ion was measured with high accuracy [1]. Due to the high Z value the frequency of the transition between the $F=5$ and $F=4$ hyperfine sublevels is in the optical region. This allowed for the use of the optical laser pumping of the $^{209}_{83}$Bi ions in the ground state circulating in the large storage ring at GSI, Darmstadt, and the observation of the subsequent fluorescence. This measurement was a challenge for the theoreticians, since usually the hfs calculations in heavy neutral atoms require, apart from the fully relativistic approach, mainly the proper treatment of the correlation effects [2]. In contrast to neutral atoms, in highly charged ions the correlation plays only a minor role, but quantum electrodynamical (QED) and nuclear structure effects become increasingly important.

In a series of theoretical studies of the hfs for $^{209}_{83}Bi^{82+}$ ion in the ground state the Bohr-Weisskopf (or magnetic dipole) distribution [3–5], the vacuum polarization (VP) [6,7], and electron self-energy [7–9] QED corrections were calculated. The calculations of the hfs for Li-like $^{209}_{83}Bi^{80+}$ ions were also performed without QED corrections but with the inclusion of the interelectron interaction [10] and correlation corrections [11]. In Ref. [12] the ''dynamical'' model for the ground state hfs in $^{209}_{83}$Bi ions was proposed. In this model the $^{209}_{83}$Bi nucleus (with nuclear spin 9/2) is considered to be composed of a $^{208}_{82}$Pb nucleus (with zero nuclear spin) plus a valence proton in the ground $1h_{9/2}$ state; the latter is treated as a Dirac particle. The ''dynamical'' model takes into account explicitly the outer proton motion inside the nucleus, i.e., magnetic moment distribution and in particular the angular part of this distribution [13]. Since the outer proton is described by the Dirac equation, this model also takes into account relativistic effects in the magnetic moment distribution. The ''dynamical'' model was applied further to the $2p_{3/2}$ state of the highly charged $^{209}_{83}$Bi ions [14]. In this case, apart from the magnetic dipole ($M1$) one, the electric quadrupole ($E2$) contribution is also essential. The small contribution of magnetic octupole ($M3$) was also considered in Ref. [14]. The ''dynamical'' model includes automatically the $E2$ moment distribution inside the nucleus.

The compilation of the results of all the works mentioned above is given in Table I. As can be seen from this table, the effect of electron relativity is the most significant. Particularly, in the case of s states, the electron relativistic corrections turn out to be the same order of magnitude as the corresponding values for the nonrelativistic hfs splittings. Corrections due to the nuclear charge distribution and interelectron interaction lead to less essential contributions to hfs. From Table I we can also draw the conclusion that for calculating the hfs of few-electron $^{209}_{83}$Bi ions with an accuracy of about 1% it would be sufficient to perform the ''dynamical model'' calculation using Dirac-Hartree-Fock (DHF) wave functions. The Breit interelectron interaction could be included in the DHF scheme in the simplified form

$$V_{\mathrm{Br}}=-\frac{1}{2}\left(\frac{\boldsymbol{\alpha}_1\cdot\boldsymbol{\alpha}_2}{r_{12}}+\frac{(\boldsymbol{\alpha}_1\cdot\mathbf{r}_{12})(\boldsymbol{\alpha}_2\cdot\mathbf{r}_{12})}{r_{12}^3}\right),$$

which is obtained in the low-frequency limit. Here $\boldsymbol{\alpha}_i$ are the Dirac matrices for two electrons and $r_{12}=|\mathbf{r}_{12}|=|\mathbf{x}_1-\mathbf{x}_2|$.

*Electronic address: anef@thd.pnpi.spb.ru

TABLE I. Relative importance of different effects contributing to the hfs of the highly charged $^{209}_{83}$Bi ions (in %).

Effect	Electron state		
	$1s_{1/2}$	$2s_{1/2}$	$2p_{3/2}$
Electron relativity	+112 [17]	+179 [10,17]	+12 [17]
Nuclear charge distribution			
(finite nucleus versus point nucleus)	−12 [6,13]	−12 [10,13]	0 [13]
Magnetic dipole distribution	−1.5 [4]	−1.5 [10]	0 [This work][a]
Electric quadrupole distribution			0 [This work][a]
QED effects (total)	0.8 [6–9]		
Interelectron Coulomb interaction		−4 [10,11]	−6 [This work]
Interelectron Breit interaction		0.5 [10]	
Electron correlation		<0.5 [11]	
Proton relativity	3 [12]		1 [14]

[a]The corresponding values in Ref. [14] were overestimated.

The next step is the inclusion of QED corrections. The first type of these corrections, vacuum polarization, is treated in this paper in the Uehling approximation. The use of the ''dynamical'' model simplifies this treatment and allows for the inclusion of the VP correction also in the $E2$ hfs contribution.

The ''dynamical'' model description for the $^{209}_{83}$Bi nucleus is essentially a single-particle one. It is well known that the core polarization correction for the magnetic moment of the $^{209}_{83}$Bi nucleus is as large as about 40%. In the ''dynamical'' model, the valence proton is described as a Dirac particle without the anomalous magnetic moment. However, both of these corrections nearly cancel, giving in the dynamic model the relativistic gyromagnetic ratio of $g_I^{\rm rel}=0.8852$ [12], close to the experimental one, $g_I^{\rm expt}=0.9134$ [15,16].

The nuclear model that takes into account the nuclear core polarization by the valence proton was developed in Ref. [5]. The excited-core configurations were included in the nuclear wave function. The single-particle excitation energies as well as the parameters of the phenomenological model potentials necessary for the calculation of the nucleon-nucleon interactions were taken from existing experimental data. This calculation gives a very accurate value for g_I. However, the agreement with the experimental value for the $^{209}_{83}$Bi^{82+} ground-state hfs appeared to be too close, not leaving room for QED corrections (0.2% instead of 0.8% in Table I).

We should emphasize that the measurement of the $E2$ contribution to the hfs of $^{209}_{83}$Bi ions would be of great importance because of the lack of reliable experimental values for the electric quadrupole moment Q for $^{209}_{83}$Bi nucleus. The known experimental and theoretical values for Q are listed in Table II. The deviations between the atomic Q values are entirely due to inaccuracies of the electric-field gradient. It should be also noted that the two values of Q have been obtained in Ref. [23]. However, they are not consistent with the Q values deduced in different works. From the comparison of the two theoretical values given in Table II we can see that the Q value depends on the nuclear radius, and the influence of the core polarization effects taken into account in Ref. [5] seems to be as strong as for the magnetic dipole moment.

Atomic units $\hbar=e=1$ with the fine-structure constant $\alpha=1/c$ and the electron mass m_e are used.

II. DYNAMICAL MODEL FOR THE hfs IN $^{209}_{83}$Bi IONS

The main features of the ''dynamical'' model for the hyperfine interaction in $^{209}_{83}$Bi ions are as follows [12,14]. We treat the valence proton and the electrons in $^{209}_{83}$Bi ion as a system of few interacting particles. All the particles move in the field of the nuclear core and interact with one another by exchange of photons. We use the Furry picture in QED and

TABLE II. Experimental and theoretical values for the electric quadrupole moment Q of the $^{209}_{83}$Bi nucleus (in barns).

Experiment			Theory
Muonic	Atomic	Pionic	Nuclear
−0.37(3) [18]	−0.379(15)[19]	−0.50(8) [24]	−0.35 [5]
	−0.383(40)[20]	−0.50(21)[25]	−0.277 [This work][a]
	−0.46 [21]		
	−0.41(1) [22]		
	−0.55(1) [23]		
	−0.71(1) [23]		

[a]Note that this value has been obtained within the single-particle model, assuming the nuclear multipole moments arise from the $1h_{9/2}$ proton alone. The corresponding value in Ref. [14] was overestimated.

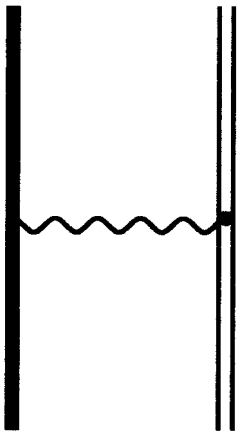

FIG. 1. Feynman graph describing the hfs interaction between the proton in the ground state $|LIM_I\rangle$ and the valence electron in the state $|nljm\rangle$. The thick line designates the proton, the double line designates the electron in the field of the core, and the wavy line designates the photon.

describe the proton as a Dirac particle moving in a central potential $U(r)$ determined by the strong interactions. The electrons are also described as Dirac particles but moving in the potential $V(r)=V_{\rm C}^{(Z-1)}(r)+V_{\rm DHF}(r)$ where $V_{\rm C}^{(Z-1)}(r)=(Z-1)\varphi(r)/r$ is the Coulomb potential of the nuclear core, corrected by the function $\varphi(r)$ for an extended nucleus, and $V_{\rm DHF}$ is the Dirac-Hartree-Fock potential.

The hfs interaction is then described by the Feynman graph of Fig. 1. This contribution to the hfs term energy can be evaluated in the Furry picture to yield

$$\Delta E^{\rm hfs}(F)=-\sum_{M_I',m'}\sum_{M_I,m}C^{Ij}_{FM_F}(M_I',m')C^{Ij}_{FM_F}(M_I,m)\times\int d\mathbf{x}_1 d\mathbf{x}_2\bar{\psi}_{LIM_I'}(\mathbf{x}_1)\bar{\psi}_{nljm'}(\mathbf{x}_2)\times\gamma_1^\mu\gamma_2^\nu\psi_{LIM_I}(\mathbf{x}_1)\psi_{nljm}(\mathbf{x}_2)D_{\mu\nu}(\mathbf{x}_1,\mathbf{x}_2;0). \tag{1}$$

Here the first variable of integration refers to the proton in the state with quantum numbers LIM_I, and second one refers to the electron in the state described by the $nljm$ set. In Eq. (1), $D_{\mu\nu}(\mathbf{x}_1,\mathbf{x}_2;\omega)=g_{\mu\nu}D(\mathbf{x}_1,\mathbf{x}_2;\omega)$ denotes the photon propagator, where $D(\mathbf{x}_1,\mathbf{x}_2;\omega)$ is given by

$$D(\mathbf{x}_1,\mathbf{x}_2;\omega)=-4\pi\int\frac{d\mathbf{k}}{(2\pi)^3}\frac{\exp[i\mathbf{k}\cdot(\mathbf{x}_1-\mathbf{x}_2)]}{(\omega/c)^2-\mathbf{k}^2+i0}. \tag{2}$$

After integrating over $\mathbf{k}$ in Eq. (2) and substituting the result in Eq. (1) we arrive at the expression used for the evaluation of the hfs in Refs. [12,14]:

$$\Delta E^{\rm hfs}(F)=-\sum_{M_I',m'}\sum_{M_I,m}C^{Ij}_{FM_F}(M_I',m')C^{Ij}_{FM_F}(M_I,m)\times\left\langle LIM_I',nljm'\left|\frac{1-\boldsymbol{\alpha}_1\cdot\boldsymbol{\alpha}_2}{r_{12}}\right|LIM_I,nljm\right\rangle. \tag{3}$$

The term with the $\boldsymbol{\alpha}$ matrices in Eq. (3) is responsible for the magnetic multipole interactions [12] and the term without the $\boldsymbol{\alpha}$ matrices is responsible for the electric multipole interactions [14]. It is important to mention that in the multipole expansion of the term without the $\boldsymbol{\alpha}$ matrices the monopole contribution should be omitted, since it corresponds to the Coulomb interaction of the electron with the electric charge of the outer proton and thus is included in the electron wave functions. Then we should consider higher-order ladder graphs that contain the interaction

$$V^{\rm hfs}=-\frac{(1-\boldsymbol{\alpha}_1\cdot\boldsymbol{\alpha}_2)}{r_{12}}+\frac{1}{r_2} \tag{4}$$

once and many times the term $-V_{\rm C}=-1/r_2$ that represents the Coulomb interaction between the proton and the electron. As demonstrated in Ref. [12], the summation of these terms up to infinite order leads to the replacement of the electron wave function for the potential $V_{\rm C}^{(Z-1)}(r)$ in Eq. (3) by the wave function for the electron in the corresponding potential $V_{\rm C}^{(Z)}(r)$. Below, we assume that this substitution has been accomplished.

The angular integration in Eq. (3) was performed for the general case in Refs. [12,14]. The magnetic contribution to $\Delta E^{\rm hfs}(F)$ according to Ref. [12] reads

$$\Delta E^{\rm hfs}_{\rm M}(F)=\sum_{\lambda=1}^{\infty}\Delta E^{\rm hfs}_{{\rm M}\lambda}(F)=\sum_{\lambda=1}^{\infty}(-1)^{I+j+F+\lambda}\begin{Bmatrix}IjF\\ jI\lambda\end{Bmatrix}N_\lambda(I,j)Q_\lambda(K,\kappa), \tag{5}$$

where

$$N_\lambda(I,j)=(-1)^\lambda\frac{4K\kappa}{\lambda(\lambda+1)}C_\lambda(I)C_\lambda(j), \tag{6}$$

$$C_\lambda(j)=(-1)^{j+1/2}(2j+1)\begin{pmatrix}j & \lambda & j\\ 1/2 & 0 & -1/2\end{pmatrix}\quad(\lambda\ \text{odd}), \tag{7}$$

$$C_\lambda(j)=0\quad(\lambda\ \text{even}). \tag{8}$$

Here $K=(L-I)(2I+1)$ and $\kappa=(l-j)(2j+1)$ are the relativistic quantum numbers for the proton and electron, respectively.

The radial integral $Q_\lambda(K,\kappa)$ is determined by

$$Q_\lambda(K,\kappa)=\int_0^\infty dr\int_0^\infty dr'\,\frac{r_<^\lambda}{r_>^{\lambda+1}}[2g_K(r)f_K(r)]$$
$$\times[2g_{n\kappa}(r')f_{n\kappa}(r')], \tag{9}$$

where $g_K(r)$ and $f_K(r)$ are the large and small components of the proton wave function, respectively, whereas $g_{n\kappa}(r)$ and $f_{n\kappa}(r)$ represent the upper and lower components of the electron wave function.

The electric contribution to $\Delta E^{\rm hfs}(F)$ according to Ref. [14] looks like

$$\Delta E_{\rm E}^{\rm hfs}(F)=\sum_{\lambda=2}^{\infty}\Delta E_{{\rm E}\lambda}^{\rm hfs}(F)=\sum_{\lambda=2}^{\infty}(-1)^{F+\lambda}\begin{Bmatrix} IjF \\ jI\lambda\end{Bmatrix}T_\lambda(I,j)R_\lambda(K,\kappa), \tag{10}$$

where

$$T_\lambda(I,j)=(-1)^{I+j+1}\left[\frac{(\lambda-1)!!}{\lambda!!}\right]^2\left[\frac{(2I+\lambda+1)!!(2j+\lambda+1)!!(2I-\lambda)!!(2j-\lambda)!!}{(2I-\lambda-1)!!(2j-\lambda-1)!!(2I+\lambda)!!(2j+\lambda)!!}\right]^{1/2} \tag{11}$$

for even λ, and $T_\lambda(I,j)=0$ for odd λ. The radial integral reads

$$R_\lambda(K,\kappa)=\int_0^\infty dr\int_0^\infty dr'\,\frac{r_>^\lambda}{r_<^{\lambda+1}}[g_K^2(r)+f_K^2(r)][g_{n\kappa}^2(r')+f_{n\kappa}^2(r')]. \tag{12}$$

The magnetic dipole contribution follows from Eq. (5) for $\lambda=1$:

$$\Delta E_{\rm M1}^{\rm hfs}(F)=\tfrac{1}{2}aC, \tag{13}$$

where the cosine factor $C=F(F+1)-I(I+1)-j(j+1)$ and the hyperfine constant a is given by

$$a=\frac{\kappa K}{2I(I+1)j(j+1)}Q_1(K,\kappa). \tag{14}$$

The electric quadrupole contribution follows from Eq. (10) for $\lambda=2$:

$$\Delta E_{\rm E2}^{\rm hfs}(F)=\Delta+bC(C+1), \tag{15}$$

where $\Delta=-4I(I+1)j(j+1)b/3$ and the hyperfine structure constant b is defined as

$$b=-\frac{3}{32}\,\frac{1}{I(I+1)j(j+1)}R_2(K,\kappa). \tag{16}$$

III. VACUUM-POLARIZATION CORRECTIONS TO THE hfs IN THE UEHLING APPROXIMATION

The evaluation of radiative corrections to the hfs in the framework of the ''dynamical'' model looks straightforward due to the direct applicability of the standard bound state QED methods. The lowest-order electron self-energy radiative corrections correspond to the Feynman graphs of Fig. 2. The lowest-order vacuum-polarization corrections correspond to the Feynman graphs of Fig. 3.

The graphs of Figs. 2 and 3 are analogous to the graphs that describe the radiative corrections to the interelectron interaction in highly charged ions. The contributions of all these graphs to the ground-state Lamb shift in two-electron highly charged ions were calculated recently [26,27]. The analogous calculation could be pursued for the graphs Figs. 2 and 3 as well. In this paper we will, however, restrict ourselves to the calculation of the VP radiative correction. In this case very accurate results can be obtained in the so-called Uehling approximation. This approximation was used for calculating the VP radiative correction to the ground-

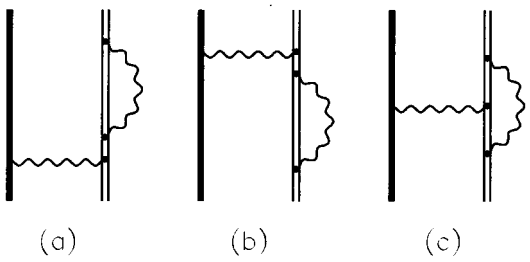

FIG. 2. Feynman graphs corresponding to the radiative electron self-energy corrections to the hfs in the ''dynamical'' model.

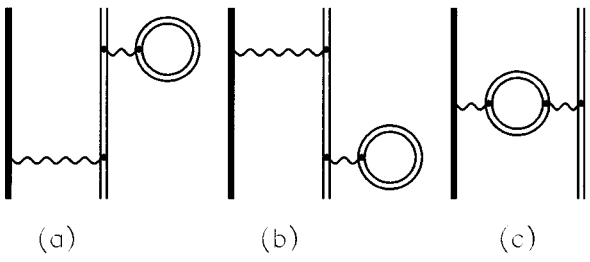

FIG. 3. Feynman graphs corresponding to the radiative vacuum polarization corrections to the hfs in the ''dynamical'' model.

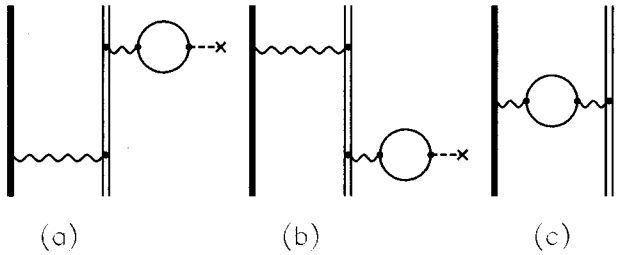

FIG. 4. Feynman graphs corresponding to the vacuum polarization corrections in the Uehling approximation. The ordinary solid line denotes the free electron and the dashed line with the cross at the end denotes the interaction with the nuclear Coulomb potential. The other notations are the same as in Figs. 1, 2, and 3.

state hfs of $^{209}_{83}\mathrm{Bi}^{82+}$ ion in Ref. [6] and its inaccuracy was proven to be about 2% [7].

In the Uehling approximation the vacuum electron loop is expanded in powers of the nuclear potential [point-nucleus Coulomb potential Z/r or extended nucleus potential $V_{\mathrm{C}}^{(Z)}(r)$]. We will use the potential Z/r since the total inaccuracy induced by this choice in the hfs calculations will be less than 0.1% (see Table I). The expansion in powers of the nuclear potential is equivalent to the expansion in powers of αZ, but for the closed electron loops the expansion parameter is actually $(\alpha Z/\pi)^2$.

In the Uehling approximation the Feynman graphs in Fig. 3 should be replaced by the graphs in Fig. 4. Let us consider first the graphs in Figs. 4(a) and 4(b). As proposed in Ref. [6], these graphs can be calculated by adding the Uehling potential directly to the DHF equations for the wave functions. The Uehling potential can be expressed as (see, for example, [28])

$$V_{\mathrm{Ueh}}(r)=\frac{2\alpha}{3\pi}\frac{Z}{r}\int_1^\infty d\zeta\left(1+\frac{1}{2\zeta^2}\right)\frac{\sqrt{\zeta^2-1}}{\zeta^2}e^{-2m_e c r\zeta}. \tag{17}$$

The net contribution can be obtained by subtracting from these results the corresponding results without the V_{Ueh} term.

The evaluation of the contribution in Fig. 4(c) looks more complicated. In Ref. [6] this problem was solved for the $M1$ hfs interaction in the ''external field'' limit. In this paper we solve this problem for all magnetic and electric hfs interactions within the ''dynamical'' model. We will use an approach developed in Ref. [29], replacing the photon propagator (2) by the renormalized second-order photon propagator, which in the Feynman gauge can be written as [30]

$$\widetilde{D}(\mathbf{x}_1,\mathbf{x}_2;\omega)=4\pi\frac{\alpha}{\pi}\int\frac{d\mathbf{k}}{(2\pi)^3}e^{i\mathbf{k}\cdot(\mathbf{x}_1-\mathbf{x}_2)}\times\int_0^1 dv\,\frac{v^2(1-v^2/3)}{4m_e^2c^2-(1-v^2)[(\omega/c)^2-\mathbf{k}^2]}. \tag{18}$$

The integration over $\mathbf{k}$ in Eq. (18) can be performed explicitly. We present here the result for the propagator $\widetilde{D}(\mathbf{x}_1,\mathbf{x}_2;0)$ that enters in Eq. (1):

$$\widetilde{D}(\mathbf{x}_1,\mathbf{x}_2;0)=\frac{1}{r_{12}}\frac{\alpha}{\pi}\int_0^1 dv\frac{v^2(1-v^2/3)}{(1-v^2)}e^{-(2m_e c/\sqrt{1-v^2})r_{12}}=\frac{1}{r_{12}}\frac{2\alpha}{3\pi}\int_1^\infty d\zeta\left(1+\frac{1}{2\zeta^2}\right)\frac{\sqrt{\zeta^2-1}}{\zeta^2}e^{-2m_e c\zeta r_{12}}. \tag{19}$$

For the integration over angles we can employ the expansion [31,32]

$$\frac{e^{-\xi r_{12}}}{r_{12}}=\frac{4\pi}{\sqrt{r_1 r_2}}\sum_{\lambda=0}^{\infty}I_{\lambda+1/2}(\xi r_<)K_{\lambda+1/2}(\xi r_>)\sum_{m=-\lambda}^{\lambda}Y^*_{\lambda m}(\Omega_1)Y_{\lambda m}(\Omega_2), \tag{20}$$

where $I_{\lambda+1/2}$ and $K_{\lambda+1/2}$ are modified Bessel and Hankel functions, respectively.

Note that we actually have to use the Coulomb gauge for the photon propagator to be able to separate out magnetic and electric contributions to the hyperfine interaction. However, the diagonal matrix elements of the potential (4) are gauge invariant [33] and in lowest order this separation is not necessary. The same is valid for the interaction modified by the vacuum polarization. Then all the formulas in Sec. II but Eqs. (9) and (12) remain unchanged. The radial integrals Q_λ and R_λ for magnetic and electric contributions now become

$$\widetilde{Q}_\lambda(K,\kappa)=(2\lambda+1)\frac{2\alpha}{3\pi}\int_1^\infty d\zeta\left(1+\frac{1}{2\zeta^2}\right)\frac{\sqrt{\zeta^2-1}}{\zeta^2}\int_0^\infty dr\int_0^\infty dr'\,\frac{1}{\sqrt{rr'}}I_{\lambda+1/2}(2m_e c\zeta r_<)K_{\lambda+1/2}(2m_e c\zeta r_>)[2g_K(r)f_K(r)]\times[2g_{n\kappa}(r')f_{n\kappa}(r')], \tag{21}$$

$$\widetilde{R}_\lambda(K,\kappa)=(2\lambda+1)\frac{2\alpha}{3\pi}\int_1^\infty d\zeta\left(1+\frac{1}{2\zeta^2}\right)\frac{\sqrt{\zeta^2-1}}{\zeta^2}\int_0^\infty dr\int_0^\infty dr'\,\frac{1}{\sqrt{rr'}}I_{\lambda+1/2}(2m_e c\zeta r_<)K_{\lambda+1/2}(2m_e c\zeta r_>)[g_K^2(r)+f_K^2(r)]\times[g_{n\kappa}^2(r')+f_{n\kappa}^2(r')]. \tag{22}$$

With the derivation of these formulas the scheme for the $^{209}_{83}$Bi ions is completed.

IV. EXTERNAL FIELD LIMIT

In the external field limit we assume that $r \ll r'$ in the radial integrals (21) and (22), and retain only the leading terms in the expansion over r/r'. Note that the integrals (21) and (22) factorize in this limit. Then we obtain the following expressions for these integrals:

$$\widetilde{Q}_1^{\rm ext}(K,\kappa)=\frac{2\alpha}{3\pi}\int_0^\infty dr r[2g_K(r)f_K(r)]\int_0^\infty dr'\frac{1}{r'^2}[2g_{n\kappa}(r')f_{n\kappa}(r')]\int_1^\infty d\zeta\left(1+\frac{1}{2\zeta^2}\right)\frac{\sqrt{\zeta^2-1}}{\zeta^2}(1+2m_e c r'\zeta)e^{-2m_e c r'\zeta}, \tag{23}$$

$$\widetilde{R}_2^{\rm ext}(K,\kappa)=\frac{2\alpha}{3\pi}\int_0^\infty dr r^2[g_K^2(r)+f_K^2(r)]\int_0^\infty dr'\frac{1}{r'^3}[g_{n\kappa}^2(r')+f_{n\kappa}^2(r')]\int_1^\infty d\zeta\left(1+\frac{1}{2\zeta^2}\right)\frac{\sqrt{\zeta^2-1}}{\zeta^2}$$
$$\times\left(1+2m_e c r'\zeta+\frac{(2m_e c r'\zeta)^2}{3}\right)e^{-2m_e c r'\zeta} \tag{24}$$

in the case of the magnetic dipole and electric quadrupole contributions, respectively. Using the definitions [14] for the nuclear magnetic dipole moment

$$\mu=-\frac{K}{(2I+2)}\int_0^\infty dr r[2g_K(r)f_K(r)] \tag{25}$$

and for the nuclear electric quadrupole moment

$$Q=-\frac{(2I-1)}{(2I+2)}\int_0^\infty dr r^2[g_K^2(r)+f_K^2(r)], \tag{26}$$

we can rewrite Eqs. (23) and (24) in the form

$$\widetilde{Q}_1^{\rm ext}(K,\kappa)=-\frac{2\alpha}{3\pi}\frac{(2I+2)}{K}\mu\int_0^\infty dr\frac{1}{r^2}[2g_{n\kappa}(r)f_{n\kappa}(r)]\int_1^\infty d\zeta\left(1+\frac{1}{2\zeta^2}\right)\frac{\sqrt{\zeta^2-1}}{\zeta^2}(1+2m_e c r\zeta)e^{-2m_e c r\zeta}, \tag{27}$$

$$\widetilde{R}_2^{\rm ext}(K,\kappa)=-\frac{2\alpha}{3\pi}\frac{(2I+2)}{(2I-1)}Q\int_0^\infty dr\frac{1}{r^3}[g_{n\kappa}^2(r)+f_{n\kappa}^2(r)]\int_1^\infty d\zeta\left(1+\frac{1}{2\zeta^2}\right)\frac{\sqrt{\zeta^2-1}}{\zeta^2}\left(1+2m_e c r\zeta+\frac{(2m_e c r\zeta)^2}{3}\right)e^{-2m_e c r\zeta}. \tag{28}$$

Equation (27) slightly differs from the corresponding expression given in Ref. [6] for the vacuum polarization correction to the hyperfine-structure splitting. There is an extra factor 2 in the first bracket of the Eq. (12) in Ref. [6], which should be absent. However, we should note that the numerical results listed in Ref. [6] are in agreement with our calculations. The correction given by Eq. (28) has never been discussed.

V. NUMERICAL RESULTS AND DISCUSSION

For the numerical calculations we use solutions of the Dirac equation for the proton with the Saxon-Woods potential

$$U(r)=-\frac{V_0}{\exp[(r-c_1)/a_1]+1} \tag{29}$$

with $c_1=r_0A^{1/3}$ fm and $a_1=0.5$ fm [34]. The parameters $V_0=33.8797$ MeV and $r_0=1.2065$ fm were chosen, as in Ref. [12], to yield the experimental binding energy $E_p=3.7977$ MeV [34] for the valence proton in the ground $1h_{9/2}$ state and to give $R_{\rm rms}=6.177$ fm. This latter value is the root-mean-square radius of the magnetization distribution from a nuclear mean-field calculation obtained in Ref. [4]. The electron Dirac and DHF wave functions are evaluated in the field of a finite charge distribution defined by the charge density function,

$$\rho(r)=\frac{\rho_0}{\exp[(r-c_2)/a_2]+1} \tag{30}$$

with $c_2=6.75$ fm and $a_2=0.468$ fm [35].

Within the DHF approach [36] and the dynamical proton model, we have calculated the hfs splitting of the ground state of the lithiumlike $^{209}_{83}$Bi ion. Without taking into account the one-electron radiative corrections, our value of $\lambda=1.553$ μm agrees quite well with $\lambda=1.543(11)$ μm obtained in Ref. [10] and experimental value $\lambda^{\rm exp}=1.544(57)$ μm reported in Ref. [37]. It should be noted that we scaled

TABLE III. Different contributions of the vacuum polarization correction to the $M1$ hfs splitting of the ground states in H- and Li-like bismuth ions (in eV).

Effect	$1s_{1/2}$	$2s_{1/2}$
Uehling correction of the wave function	0.0260 [6]	0.0041
Uehling-like loop correction	0.0093 [6]	0.0015
Wichmann-Kroll correction of the wave function	−0.0007 [7]	
Total vacuum polarization contribution	0.0346 [7]	0.0056

our result by the ratio of the observed magnetic moment to the calculated moment. In addition, here we took into account the small Breit interaction contribution, which was taken from Ref. [10]. We also calculated the vacuum polarization contribution to the hfs splitting of the ground state in $^{209}_{83}\mathrm{Bi}^{80+}$ ions (see Table III). The first line in Table III corresponds to a calculation of the graphs in Figs. 4(a) and 4(b), and the second line corresponds to the contribution from the graph in Fig. 4(c). We have not calculated the Wichmann-Kroll corrections, which are estimated to be quite small [7]. The more important electron self-energy correction remains still to be compiled.

The dynamical proton model in combination with the DHF method has also been applied for the calculation of the hyperfine splittings of $2p_{3/2}$ states in lithium-, boron-, and nitrogen-like bismuth ions. The binding energies for the outer $2p_{3/2}$ electron for $^{209}_{83}\mathrm{Bi}^{80+}$, $^{209}_{83}\mathrm{Bi}^{78+}$, and $^{209}_{83}\mathrm{Bi}^{76+}$ ions are found to be $E_e=22.8879$ keV, $E_e=22.1664$ keV, and $E_e=21.3296$ keV, respectively. The Breit interaction as well as correlation corrections were not included in the calculations. The results of our evaluations for Li-like, B-like, and N-like ions are summarized in Tables IV, V, and VI, respectively. The first line in Tables IV, V, and VI for both $M1$ and $E2$ contributions corresponds to calculations with pure Dirac wave functions. Effects connected with the magnetic dipole and electric quadrupole distributions turn out to be negligible. The second line corresponds to the difference between the calculations with DHF and pure Dirac wave functions. The third line is the net contribution of the vacuum polarization correction calculated in the Uehling approximation. Since the $M3$ contribution is quite small, only the total value without the VP correction is given. The values of $M1$ contributions were normalized to the known experimental value of the magnetic nuclear moment [15,16], and the values of $E2$ contributions were normalized to the pionic Q value of $-0.500(80)$ b selected for the ''1992'' set of moments [38]. As seen from the tables, the VP contributions to the hfs splittings of $2p_{3/2}$ states turn out to be very small. The remaining part of the QED corrections (electron self-energy correction) requires special treatment. A further improvement of the theory should incorporate the inclusion of the ''dynamical'' model in the multiconfigurational Dirac-Fock scheme for taking into account the electron correlation. Correlation corrections could be more essential for N-like ions. This inclusion seems to be relatively straightforward. The other improvement concerns the nuclear core polarization effect. This work can be performed along the lines indi-

TABLE IV. Contribution of various effects to the hfs splittings $\Delta E^{\mathrm{hfs}}(F)-\Delta E^{\mathrm{hfs}}(F')$ of the $2p_{3/2}$ state in $^{209}_{83}\mathrm{Bi}^{80+}$ ions (in meV).

	Effect	F,F' 6, 5	5, 4	4, 3
$M1$	First order	30.760	25.633	20.506
	Interelectron Coulomb interaction	−1.816	−1.513	−1.210
	Vacuum polarization	0.002	0.002	0.002
	Total	28.946	24.122	19.298
$E2$	First order	−3.813	1.192	3.813
	Interelectron Coulomb interaction	0.235	−0.075	−0.235
	Vacuum polarization	−0.001	0	0.001
	Total	−3.579	1.117	3.579
$M3$	Total	0.001	−0.001	0.001
	Total splitting	25.368	25.238	22.878

TABLE V. Contribution of various effects to the hfs splittings $\Delta E^{\mathrm{hfs}}(F)-\Delta E^{\mathrm{hfs}}(F')$ of the $2p_{3/2}$ state in $^{209}_{83}\mathrm{Bi}^{78+}$ ions (in meV).

	Effect	F,F' 6, 5	5, 4	4, 3
$M1$	First order	30.760	25.633	20.506
	Interelectron Coulomb interaction	−2.431	−2.025	−1.620
	Vacuum polarization	0.002	0.002	0.002
	Total	28.331	23.610	18.888
$E2$	First order	−3.813	1.192	3.813
	Interelectron Coulomb interaction	0.314	−0.098	−0.314
	Vacuum polarization	−0.001	0.	0.001
	Total	−3.500	1.094	3.500
$M3$	Total	0.001	−0.001	0.001
	Total splitting	24.832	24.703	22.389

TABLE VI. Contribution of various effects to the hfs splittings $\Delta E^{\mathrm{hfs}}(F)-\Delta E^{\mathrm{hfs}}(F')$ of the $2p_{3/2}$ state in $^{209}_{83}\mathrm{Bi}^{76+}$ ions (in meV).

	Effect	F,F' 6, 5	5, 4	4, 3
$M1$	First order	30.760	25.633	20.506
	Interelectron Coulomb interaction	−3.233	−2.694	−2.155
	Vacuum polarization	0.002	0.002	0.002
	Total	27.529	22.941	18.353
$E2$	First order	−3.813	1.192	3.813
	Interelectron Coulomb interaction	0.416	−0.131	−0.416
	Vacuum polarization	−0.001	0.	0.001
	Total	−3.398	1.061	3.398
$M3$	Total	0.001	−0.001	0.001
	Total splitting	24.132	24.001	21.752

cated in Ref. [39] for the nuclear polarization by the electrons.

Concerning the possible experimental perspectives in this direction we must admit that probably the best opportunity would be given by the N-like $^{209}_{83}\mathrm{Bi}^{76+}$ ion, where the $(1s)^2(2s)^2(2p_{1/2})^2 2p_{3/2}$ state is the ground state [14]. The frequency of the transition $(F=6 \rightarrow F=5)$ from the highest hfs sublevel is about 24.132 meV (far infrared) and the lifetime of the $F=6$ state is of the order of 1 h. Assuming that in the GSI storage ring 10^8 ions can circulate during 1 h [1] and that for achieving the accuracy 10^{-2} the statistics would require 10^4 events, the efficiency of the detector not less than 10^{-4} would be required for the emission measurement. The other problem is that suitable lasers are absent in the far infrared; the alternative source for the excitation of $F=5 \rightarrow F=6$ transitions could be the synchrotron radiation. Another opportunity also mentioned in Ref. [14] was the B-like $^{209}_{83}\mathrm{Bi}^{78+}$ ion, where $(1s)^2(2s)^2 2p_{3/2}$ is the first excited state with the linewidth of the order 10^{-4} eV. It looks also promising to induce the hfs transitions of the $2p_{3/2}$ state at the far infrared and to observe the $2p_{3/2} \rightarrow 2p_{1/2}$ transitions in the x-ray domain.

ACKNOWLEDGMENTS

This work was finally accomplished during a visit of A.N. to the Technische Universität of Dresden. This visit was supported by DFG. L.L. wishes to thank the University of Helsinki for hospitality and the ESF/REHE program for support. L.L. and A.N. also acknowledge support by RFFI, Grant No. 96-02-17167. G.P. and G.S. acknowledge support by the DFG, the BMBF, and by GSI (Darmstadt). P.P. acknowledges the financial support of The Academy of Finland.

[1] I. Klaft, S. Borneis, T. Engel, B. Fricke, R. Grieser, G. Huber, T. Kühl, D. Marx, R. Neumann, S. Schröder, P. Seelig, and L. Völker, Phys. Rev. Lett. **73**, 2425 (1994).
[2] I. Lindgren and A. Rosén, Case Stud. At. Phys. **4**, 197 (1974).
[3] M. Finkbeiner, B. Fricke, and T. Kühl, Phys. Lett. A **176**, 113 (1993).
[4] S. M. Schneider, J. Schaffner, W. Greiner, and G. Soff, J. Phys. B **26**, L581 (1993).
[5] M. Tomaselli, S. M. Schneider, E. Kankeleit, and T. Kühl, Phys. Rev. C **51**, 2989 (1995).
[6] S. M. Schneider, W. Greiner, and G. Soff, Phys. Rev. A **50**, 118 (1994).
[7] H. Persson, S. M. Schneider, W. Greiner, G. Soff, and I. Lindgren, Phys. Rev. Lett. **76**, 1433 (1996).
[8] V. M. Shabaev and V. A. Yerokhin, Pis'ma Zh. Éksp. Teor. Fiz. **63**, 309 (1996) [JETP Lett. **63**, 316 (1996)].
[9] S. A. Blundell, K. T. Cheng, and J. Sapirstein, Phys. Rev. A **55**, 1857 (1997).
[10] M. B. Shabaeva and V. M. Shabaev, Phys. Rev. A **52**, 2811 (1995).
[11] S. N. Panigrahy, R. W. Dougherty, T. P. Das, and J. Andriessen, Phys. Rev. A **40**, 1765 (1989).
[12] L. N. Labzowsky, W. R. Johnson, G. Soff, and S. M. Schneider, Phys. Rev. A **51**, 4597 (1995).
[13] V. M. Shabaev, J. Phys. B **27**, 5825 (1994).
[14] L. Labzowsky, I. Goidenko, M. Gorshtein, G. Soff, and P. Pyykkö, J. Phys. B **30**, 1427 (1997).
[15] P. Raghavan, At. Data Nucl. Data Tables **43**, 189 (1989).
[16] T. Bastuğ, B. Fricke, M. Finkbeiner, and W. R. Johnson, Z. Phys. D **37**, 281 (1996).
[17] P. Pyykkö, E. Pajanne, and M. Inokuti, Int. J. Quantum Chem. **7**, 785 (1973).
[18] W. Y. Lee, M. Y. Chen, S. C. Cheng, E. R. Macagno, A. M. Rushton, and C. S. Wu, Nucl. Phys. A **180**, 14 (1972).
[19] G. Eisele, I. Koniordos, G. Müller, and R. Winkler, Phys. Lett **28B**, 256 (1968).
[20] D. A. Landman and A. Lurio, Phys. Rev. A **1**, 1330 (1970).
[21] A. Rosén, Phys. Scr. **6**, 37 (1972).
[22] Yu. I. Skovpen, Opt. Spektrosk. **50**, 236 (1981) [Opt. Spectrosc. **50**, 125 (1981)].
[23] J. Dembczyński, B. Arcimowicz, E. Stachowska, and H. Rudnicka-Szuba, Z. Phys. A **310**, 27 (1983).
[24] R. Beetz, F. W. N. De Boer, J. K. Panman, J. Konijn, P. Pavlopoulos, G. Tibell, K. Zioutas, I. Bergstrom, K. Fransson, L. Tauscher, P. Blum, R. Guigas, H. Koch, H. Poth, and L. M. Simons, Z. Phys. A **286**, 215 (1978).
[25] C. J. Batty, S. F. Biagi, R. A. J. Riddle, B. L. Roberts, G. J. Pyle, G. T. A. Squier, D. M. Asbury, and A. S. Clough, Nucl. Phys. A **355**, 383 (1981).
[26] H. Persson, S. Salomonson, P. Sunnergren, and I. Lindgren, Phys. Rev. Lett. **76**, 204 (1996).
[27] V. A. Yerokhin and V. M. Shabaev, Phys. Lett. A **207**, 274 (1995); **210**, 437 (1996); Zh. Éksp. Teor. Fiz. **110**, 74 (1996) [JETP **83**, 39 (1996)].
[28] A. I. Akhiezer and V. B. Berestetskii, *Quantum Electrodynamics* (Wiley, New York, 1965).
[29] H. Persson, I. Lindgren, L. N. Labzowsky, G. Plunien, T. Beier, and G. Soff, Phys. Rev. A **54**, 2805 (1996).
[30] N. N. Bogolyubov and D. V. Shirkov, *Introduction to the Theory of Quantized Fields* (Wiley, New York, 1959).
[31] I. S. Gradshteyn and I. M. Ryzhik, *Tables of Integrals, Series, and Products* (Academic Press, New York, 1980).
[32] D. A. Varshalovich, A. N. Moskalev, and V. K. Khersonskii, *Quantum Theory of Angular Momentum* (World Scientific, Singapore, 1988).
[33] L. Labzowsky, G. Klimchitskaya, and Yu. Dmitriev, *Relativistic Effects in the Spectra of Atomic Systems* (IOP Publishing, Bristol, 1993).
[34] J. Eisenberg and W. Greiner, *Nuclear Theory: Nuclear Models* (North-Holland, Amsterdam, 1970).
[35] H. de Vries, C. W. de Jager, and C. de Vries, At. Data Nucl. Data Tables **36**, 495 (1987).
[36] I. I. Tupitsyn kindly supplied us with his original DHF code. The description of the DHF package is given in V. F. Brattsev, G. B. Deineka, and I. I. Tupitsyn, Izv. Akad. Nauk SSSR **41**, 2655 (1977) [Bull. Acad. Sci. USSR, Phys. Ser. **41**, 173 (1977)].

[37] P. Beiersdorfer, A. Osterheld, J. Scofield, J. Crespo Lopez-Urrutia, V. Decaux, and K. Widmann, Bull. Am. Phys. Soc. **42**, 988 (1997).

[38] *CRC Handbook of Chemistry and Physics*, edited by D. R. Lide, 74th ed. (CRC Press, Boca Raton, FL, 1993).

[39] G. Plunien, B. Müller, W. Greiner, and G. Soff, Phys. Rev. A **43**, 5853 (1991).